Probing the Order-to-Chaos Region in Superdeformed ^{151}Tb and ^{196}Pb Nuclei with Continuum γ Transitions

S. Leoni,[1] G. Benzoni,[1] N. Blasi,[1] A. Bracco,[1] S. Brambilla,[1] F. Camera,[1] A. Corsi,[1] F. C. L. Crespi,[1] P. Mason,[1,2] B. Million,[1] D. Montanari,[1] M. Pignanelli,[1] E. Vigezzi,[1] O. Wieland,[1] M. Matsuo,[3] Y. R. Shimizu,[4] D. Curien,[5] G. Duchêne,[5] J. Robin,[5] P. Bednarczyk,[6] M. Castoldi,[7] B. Herskind,[8] M. Kmiecik,[6] A. Maj,[6] W. Meczynski,[6] J. Styczen,[6] M. Zieblinski,[6] K. Zuber,[6] and A. Zucchiatti[7]

[1]*Dipartimento di Fisica and INFN, Sezione di Milano,Via Celoria 16, 20133 Milano, Italy*
[2]*Laboratori Nazionali di Legnaro, Viale dell'Università 2, 35020 Legnaro (PD), Italy*
[3]*Graduate School of Science and Technology, Niigata University, Niigata 950-2181, Japan*
[4]*Department of Physics, Kyushu University, 6-10-1 Hakozaki, Higashi-ku, Fukuoka 812-8581, Japan*
[5]*IPHC-DRS, ULP, CNRS, IN2P3, 23 rue du Loess, 67037 Strasbourg, France*
[6]*The Niewodniczanski Institute of Nuclear Physics, Polish Academy of Sciences, 31-342 Krakow, Poland*
[7]*INFN sezione di Genova, Via Dodecaneso 33, 16146 Genova, Italy*
[8]*The Niels Bohr Institute, Blegdamsvej 15-17, 2100, Copenhagen, Denmark*
(Received 27 June 2008; published 30 September 2008)

The γ decay associated with the warm rotation of the superdeformed nuclei ^{151}Tb and ^{196}Pb has been measured with the EUROBALL IV array. Several independent quantities provide a stringent test of the population and decay dynamics in the superdeformed well. A Monte Carlo simulation of the γ decay based on microscopic calculations gives remarkable agreement with the data only assuming a large enhancement of the $B(E1)$ strength for 1–2 MeV γ rays, which may be related to the evidence for octupole vibrations in both mass regions.

DOI: 10.1103/PhysRevLett.101.142502 PACS numbers: 21.10.Re, 23.20.Lv, 27.70.+q, 27.80.+w

The thermally excited, rapidly rotating atomic nucleus is an ideal laboratory for studying structure properties beyond the mean field. In particular, the γ decay which cools the hot compound nucleus at high angular momentum is a powerful tool for investigating the transition from the chaotic regime around the particle binding energy to the cold, ordered system close to the yrast line [1–3]. This topic, mostly investigated in normally deformed (ND) nuclei [1,2,4–8], becomes particularly interesting and challenging, both experimentally and theoretically, in the case of very elongated systems. The study of superdeformed (SD) nuclei requires, in fact, high selectivity and high statistics, in order to focus on the small fraction of the γ decay ($\approx$ few %) which is finally trapped into the SD well and populates discrete rotational bands. At present, there is only partial experimental information available for few SD nuclei [9–13], whose interpretation is based on rather schematic models [10,12,13] or depends on several parameters [9,11].

The aim of this Letter is to make a substantial step forward in the understanding of the population and decay of warm SD nuclei in the mass regions $A = 150$ and $A = 190$, where superdeformation is a well established phenomenon, by a comparative and comprehensive study of the nuclei ^{151}Tb and ^{196}Pb. For the first time, the intensities and fluctuations of several independent observables are extracted from quasicontinuum (QC) γ-coincidence spectra. This provides strong experimental constraints on the dynamics of the γ decay flow and of the tunneling through the potential barriers between SD and ND excited states, over a wide spin range. A key point of this work is the development of a new Monte Carlo simulation of the γ-cascades in the SD well, making use of discrete levels calculated microscopically. In addition, the coupling between excited SD and ND configurations is included following Ref. [14] and making use of microscopic potential barriers [15]. It is anticipated that such a detailed study of the order-to-chaos region reveals the influence of nuclear structure effects. In particular, an enhancement in the $E1$ strength around 1–2 MeV, which could be related to octupole vibrations, is found to play an important role.

The experiments were performed at the Vivitron in Strasbourg (F) with the EUROBALL IV array [16]. The reaction used were ^{130}Te(^{27}Al, $6n$)^{151}Tb (at 155 MeV) and ^{170}Er(^{30}Si, $4n$)^{196}Pb (at 148 MeV). In both cases, a stack of two self-supporting targets (with a total thickness of ≈ 1 and 1.2 mg/cm^2, respectively) were employed. In the Tb case, the full Ge ball was used, while in the Pb experiment the low efficiency Ge detectors were replaced by 8 large volume BaF_2 scintillators to measure high energy γ rays. In both cases the γ-multiplicity was measured with an InnerBall of BGO detectors. A total of 9×10^9 and 2×10^8 fivefold and threefold events and higher were collected, respectively. The SD nuclei ^{151}Tb and ^{196}Pb were investigated in detail by discrete γ spectroscopy [17]. In both cases discrete transitions linking the SD yrast band to ND configurations were identified, and for ^{196}Pb the spin and excitation energy of the SD yrast were established

[18,19]. In this work we focus instead on the unresolved excited SD rotational bands, which form ridge and valley structures in γ-coincidence spectra. The two data sets were sorted into a number of $\gamma - \gamma$ matrices in coincidence with low-lying ND transitions of ^{151}Tb or ^{196}Pb, named Total, and in coincidence with the SD yrast band (named SD-gated). In addition, rotational planes (ROT-Plane) [20], namely, matrices obtained selecting triple coincidences with the requirement $x + y = 2z$, x, y, and z being the energies of the γ rays, were also constructed in coincidence with the nucleus of interest, in order to enhance the sensitivity to rotational correlation in the γ cascades. In all cases a condition on high-fold events ($F \geq 25$ for ^{151}Tb and $F \geq 10$ for ^{196}Pb) was imposed. For each matrix the background was subtracted by scaling the ungated spectrum by a factor corresponding to the P/T of the gating transitions and further applying the COR procedure [2], which enhances the rotational correlations. In all spectra cuts perpendicular to the main diagonal reveal the existence of ridge structures extending over a broad interval of transition energies (corresponding to the spin regions 40 to 60$\hbar$ and 10 to 40$\hbar$ for ^{151}Tb and ^{196}Pb), with a spacing between the two inner most ridges equal to $2\Delta E_\gamma = 8\hbar^2/\Im^{(2)} \approx 100$ and 80 keV, respectively, where $\Im^{(2)}$ is the moment of inertia of the SD yrast band in each nucleus. Figure 1 shows examples of such cuts for the wide spin intervals $\approx$ 48–56$\hbar$ (^{151}Tb) and $\approx$ 20–34$\hbar$ (^{196}Pb). In the case of the Total and SD-gated spectra (a),(b) and (e),(f) all known ND and SD discrete peaks (dark areas in the figures) have been subtracted by the RADWARE package [21]. The ROT-planes spectra (c) and (d) are sum of cuts taken in between the SD yrast peaks. In this case, the inner most ridge corresponds to the 2nd ridge in the Total and SD-gated matrices, and the associated spacing is equal to $4\Delta E_\gamma$.

In the first place, the intensity of the ridge structures has been evaluated and compared to the SD yrast, as shown by symbols in Fig. 2. In both ^{151}Tb and ^{196}Pb nuclei the total intensity of the 1st and 2nd ridge [panels (a),(b) and (c),(d)] is up to 3 times larger than the SD yrast population at the plateau (which collects 2% and 1.3% of the total decay-flux, respectively), pointing to the existence of several discrete unresolved SD bands decaying directly into the

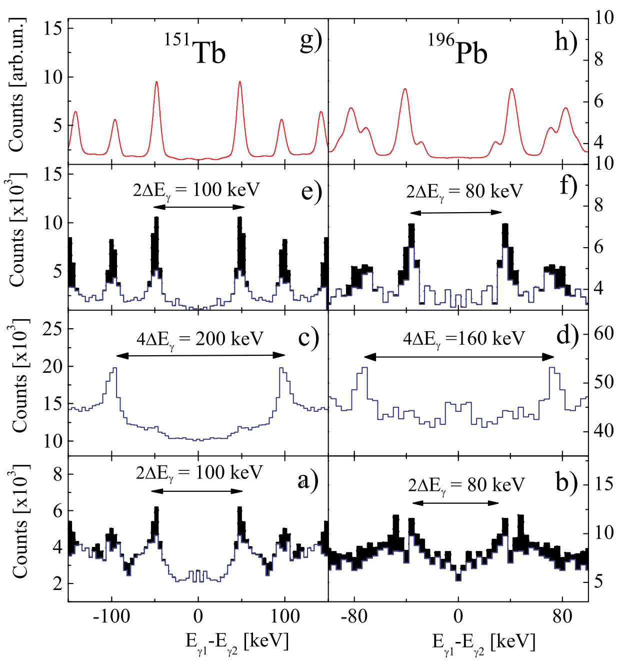

FIG. 1 (color online). Projections perpendicular to the main diagonal of γ-coincidence matrices of ^{151}Tb (left) and ^{196}Pb (right), for the energy interval 1150–1280 keV (i.e., $\approx$ 48–56$\hbar$) and 430–680 keV (i.e., 20–34$\hbar$), respectively. Panels (a),(b) show cuts on the Total matrices, (c),(d) on the rotational planes and (e),(f) on the SD-gated spectra. Simulated SD-gated spectra are given in panels (g) and (h) (see text for details).

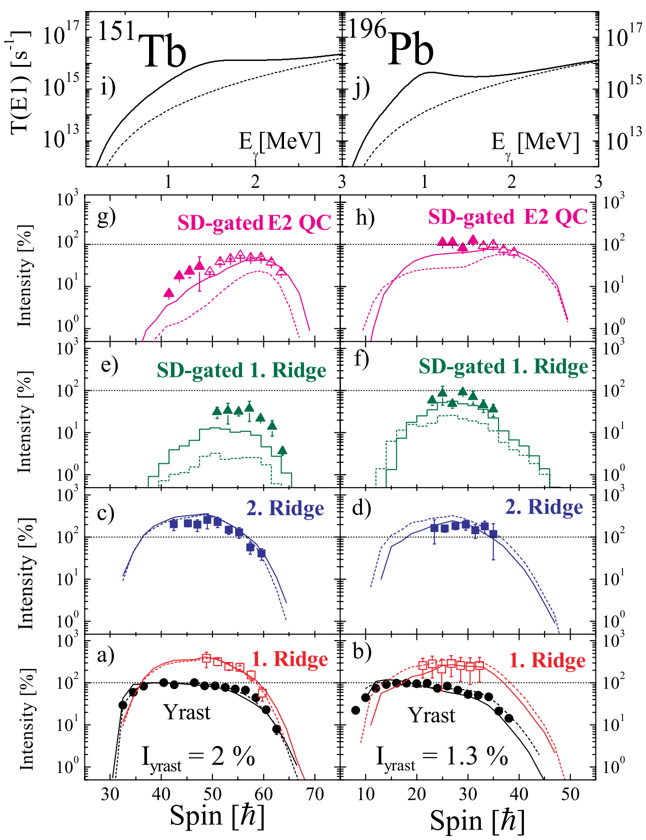

FIG. 2 (color online). Population of the excited rotational bands in the SD well of ^{151}Tb (left) and ^{196}Pb (right), relative to the corresponding SD yrast intensity (normalized to 100% at the plateau and shown by circles in the bottom panels). Data are shown by symbols: the intensities of the 1st and 2nd ridge are given in panels (a),(b) and (c),(d); panels (e),(f) refer to the SD-gated 1st ridges. Panels (g),(h) show the SD-gated $E2$ QC, with full symbols referring to data partially contaminated by $M1$'s. Predictions from simulations of the γ decay assuming a standard (enhanced) $E1$ strength [see top panels (i) and (j)] are shown by dashed (solid) lines.

low deformation minimum. The more selective analysis of the 1st ridge in coincidence with the SD yrast [panels (e) and (f)] shows that only a fraction of the SD yrast intensity (40% (80%) at $I \approx 55(25)\hbar$ in ^{151}Tb (^{196}Pb)) originates from discrete excited bands. Finally, the symbols in panels (g) and (h) give the total $E2$ QC intensity in coincidence with the SD yrast, as obtained by the analysis of the one dimensional quasicontinuum spectra in coincidence with the SD yrast band [22]. This spectrum includes both the ridge intensity and the contribution from fragmented bands at higher excitation energies, where rotational damping largely dominates [1]. In the two nuclei, the presence of contaminants (probably $M1$'s) may affect the intensities at low spins, as evidenced by full symbols in Figs. 2(g) and 2(h) [11,23]. It is found that the intensity of the SD-gated ridges accounts for almost the entire $E2$ strength up to spin $55\hbar$ in ^{151}Tb and $35\hbar$ in ^{196}Pb, corresponding to the end of the plateau regions of the SD yrast. At higher spins the ridge intensity drops to less than half of the $E2$ QC, indicating that most of the feeding of the yrast comes from damped bands. This differs from the peculiar case of ^{194}Hg, were an exceptionally narrow ridge, exhausting nearly all $E2$ decay strength has been interpreted as a signature of ergodicity in a nuclear system [13].

Additional information can be obtained from the analysis of the counts fluctuations in the γ-coincidence matrices [1,2], allowing to estimate the number of discrete bands populating the ridges. The results are shown by symbols in Fig. 3. In both cases up to more than 30 SD discrete bands are found to populate the Total ridges [(a) and (b)], half of

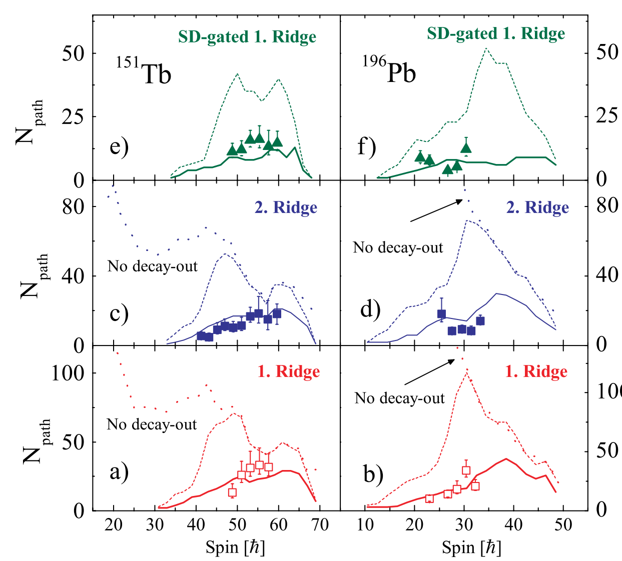

FIG. 3 (color online). The number of discrete excited SD bands obtained from the analysis of the count fluctuations of the ridge structures of ^{151}Tb (left) and ^{196}Pb (right). Panels (a), (b) and (c),(d) refer to the 1st and 2nd ridge, (e),(f) to the SD-gated 1st ridge. Symbols refer to data, solid lines to the Monte Carlo simulation. See the text for the dashed and dotted lines.

which extend at least over 3 consecutive transitions, as follows by the analysis of the 2nd ridge [(c) and (d)]. In addition, the study of the SD-gated ridges [(e) and (f)] show that no more than half of the discrete excited bands feed the SD yrast, supporting the previous analysis of the ridge intensities (see also discussion later).

The experimental findings have been compared with predictions based on a Monte Carlo simulation of the γ decay flow of ^{151}Tb and ^{196}Pb. The code is an extended version of MONTESTELLA [24] and simulates the γ decay of the excited rotating nucleus from the residual entry distribution towards the SD or the ND yrast line. It is based on the competition between $E2$ collective and $E1$ statistical transitions in both minima and on a tunneling probability across the barrier separating the two potential wells, calculated according to Ref. [14]. In the SD well energy levels, $E2$ transition probabilities and potential barriers are microscopically calculated by the cranked shell model of Refs. [15,25]. In the case of Pb, the tunneling probability includes the phenomenological adjustment $C_{mass} = 2.7$ of the mass parameter, to reproduce the decay out spin of the SD yrast. At excitation energies U above yrast higher than the ones covered by the microscopic states (i.e., $U > 4.5$ and 3.5 MeV in ^{151}Tb and ^{196}Pb, respectively) the rotational decay in the SD well proceeds through a continuum of states, governed by level densities, $E2$ strengths (with a width $\Gamma_{rot} \approx 100$, 70 keV in ^{151}Tb and ^{196}Pb, respectively) and barriers extrapolated from the microscopic region. The γ decay in the ND well is instead described schematically, with a density of states taken from Ref. [26] and a $B(E2)$ value of 30 W.u. In both wells the $E1$ decay is described by the Lorentzian strength function of the giant dipole resonance (GDR) for the corresponding deformation. An hindrance factor is used, taken from Ref. [24] in the ND well, and tuned to reproduce the intensity of the SD yrast in the SD well. The residual entry distributions for the γ decay of ^{151}Tb and ^{196}Pb have been calculated determining the fusion cross sections of the compound nuclei ^{157}Tb and ^{200}Pb [27], and then simulating the neutron evaporation by the Monte Carlo version of the code CASCADE [28]. Finally, a correction for the experimental multiplicity requirement has been included, leading to distributions with a maximum at $I = 60$ and $42\hbar$ and $U = 8.3$ and 7.7 MeV, for ^{151}Tb and ^{196}Pb, respectively. Once the entry distribution of the γ decay is defined, the use of microscopically calculated quantities leaves no room in the SD well for adjustable parameters, except for the $E1$ transition probability.

The Monte Carlo simulation provides predictions for all the observables shown in Figs. 1–3, including, for the first time, the intensity and the number of discrete bands in coincidence with the SD yrast, which depend strongly on the competition between $E2$ and $E1$ transitions along the cascades. For both nuclei the model reproduces rather well the line shape of the γ spectrum [see Figs. 1(g) and 1(h)], the SD yrast intensity and the population of the discrete excited bands forming the 1st and 2nd ridge [dashed lines in Figs. 2(a)–2(d)]. On the other hand, it largely underestimates the intensity observed in the 1st ridge and $E2$ QC in coincidence with the SD yrast [dashed lines in panels (e),(f) and (g),(h)]. These observables, although referring to the warm rotation in the transition region between order and chaos, are in fact very sensitive to the delicate balance between $E2$ and $E1$ transitions at low excitation energy, where nuclear structure effects play a major role. It is worth noticing that in both $A = 150$ and $A = 190$ mass regions, experimental evidence has been found for octupole vibrations in SD nuclei (^{152}Dy [29], ^{196}Pb [30], ^{190}Hg [31]), resulting in strongly enhanced $E1$ transitions, linking the excited SD bands to yrast. The $B(E1)$ values are in fact of the order of 10^{-4} W.u., namely, 1 to 2 orders of magnitude larger than expected from the tail of the GDR, in agreement with various theoretical models [32,33]. We have therefore performed simulation calculations for ^{151}Tb and ^{196}Pb making use of a GDR strength with an extra component giving rise to an enhancement in the $B(E1)$ values between 10 to 100, for $E1$ γ-rays of energies around 1.5 and 1 MeV, respectively, [see Figs. 2(i) and 2(j)], i.e., consistent with the values of the $E1$ enhanced transitions experimentally observed. The obtained results (solid lines in Fig. 2) are now in much better agreement with the data. The number of paths $N_{\text{path}} = 1/\sum w_i^2$, where w_i indicates the relative population w_i of each path, is also in good agreement with the data (solid lines in Fig. 3). This quantity represents a crucial test for various aspects of our model. N_{path} gives the number of discrete bands which are populated sufficiently strongly and it is determined by the level density, by the onset of damping (taking place at $U \approx 2(3)$ MeV in ^{196}Pb (^{151}Tb)) and by the population mechanism. The latter favors low-lying bands around 1–1.5 MeV, not only because they tunnel less easily through the potential barrier but also because they receive stronger $E1$ feeding. We note that N_{path} is much lower than the number of discrete bands N_{band} obtained from the cranked shell model ignoring the flow (dotted lines in Fig. 3): taking into account the depopulation of the bands due to the tunneling (as estimated in Ref. [15]) decreases N_{band} at low spins but still largely overestimates the data (dashed lines). This is different from the case of ND nuclei, where discrete bands are more equally populated and N_{path} is closer to N_{band} [24].

In summary, we have presented a study of the warm rotation in the SD nuclei ^{151}Tb and ^{196}Pb, providing a series of independent quantities which test our understanding of the γ decay in the SD well over the whole spin range. A Monte Carlo code, based on microscopic quantities, is able to reproduce all the observables except the $E2$ strength gated on the SD yrast. Better agreement can be obtained only by increasing the $E1$ strength around 1 MeV by almost 2 orders of magnitude, as compared to standard parametrizations. This may be related to the observation of strong $E1$ transitions between discrete bands, associated with octupole vibrations. Therefore, the study of the warm rotation in the transition region between order and chaos is not only instrumental in shedding light on nuclear structure properties beyond mean field, but can also be considered as a tool to unravel microscopic features of the γ decay.

This work was partially supported by EU (Contract No. EUROVIV: HPRI-CT-1999-00078) and by the Polish Ministry of Science and Higher Education (Grant No. 1-P03B-030-30).

[1] A. Bracco and S. Leoni, Rep. Prog. Phys. **65**, 299 (2002).
[2] T. Døssing *et al.*, Phys. Rep. **268**, 1 (1996).
[3] T. L. Khoo, in *Tunneling in Complex Systems*, edited by S. Tomsovic (World Scientific, Singapore, 1998), p. 229.
[4] G. Benzoni *et al.*, Phys. Lett. B **615**, 160 (2005).
[5] S. Leoni *et al.*, Phys. Rev. Lett. **93**, 022501 (2004).
[6] S. Leoni *et al.*, Phys. Rev. C **72**, 034307 (2005).
[7] F. S. Stephens *et al.*, Phys. Rev. Lett. **94**, 042501 (2005).
[8] V. Martin *et al.*, Phys. Rev. C **51**, 3096 (1995).
[9] S. Leoni *et al.*, Phys. Lett. B **409**, 71 (1997).
[10] S. Leoni *et al.*, Phys. Lett. B **498**, 137 (2001).
[11] T. Lauritsen *et al.*, Phys. Rev. C **75**, 064309 (2007).
[12] G. Benzoni *et al.*, Phys. Rev. C **75**, 047301 (2007).
[13] A. Lopez-Martens *et al.*, Phys. Rev. Lett. **100**, 102501 (2008).
[14] K. Schiffer *et al.*, Z. Phys. A **332**, 17 (1989).
[15] K. Yoshida *et al.*, Nucl. Phys. **A696**, 85 (2001).
[16] J. Simpson, Z. Phys. A **358**, 139 (1997).
[17] B. Singh *et al.*, "Table of Superdeformed Nuclear Bands and Fission Isomers" (2002).
[18] J. Robin *et al.*, Phys. Rev. C **77**, 014308 (2008).
[19] A. Wilson *et al.*, Phys. Rev. Lett. **95**, 182501 (2005).
[20] S. Leoni *et al.*, Eur. Phys. J. A **4**, 229 (1999).
[21] D. C. Radford, Nucl. Instrum. Methods Phys. Res., Sect. A **361**, 297 (1995).
[22] S. Leoni *et al.* (to be published).
[23] T. Lauritsen *et al.*, Phys. Rev. C **62**, 044316 (2000).
[24] A. Bracco *et al.*, Phys. Rev. Lett. **76**, 4484 (1996).
[25] K. Yoshida *et al.*, Nucl. Phys. **A636**, 169 (1998).
[26] S. Goriely *et al.*, At. Data Nucl. Data Tables **77**, 311 (2001).
[27] A. Winther, Nucl. Phys. **A594**, 203 (1995).
[28] F. Pulhofer, Nucl. Phys. **A280**, 267 (1977).
[29] T. Lauritsen *et al.*, Phys. Rev. Lett. **89**, 282501(2002).
[30] D. Roßbach *et al.*, Phys. Lett. B **513**, 9 (2001).
[31] B. Crowell *et al.*, Phys. Rev. C **51**, R1599 (1995); A. Korichi *et al.*, Phys. Rev. Lett. **86**, 2746 (2001).
[32] J. Kvasil *et al.*, Phys. Rev. C **75**, 034306 (2007).
[33] T. Nakatsukasa *et al.*, Phys. Lett. B **343**, 19 (1995).